Excitation of transverse dipole and quadrupole modes in a pure ion plasma in a linear Paul trap to study collective processes in intense beams[a)]

Erik P. Gilson,[1,b)] Ronald C. Davidson,[1] Philip C. Efthimion,[1] Richard Majeski,[1] Edward A. Startsev,[1] Hua Wang,[1] Stewart Koppell,[2] and Matthew Talley[3]
[1]*Plasma Physics Laboratory, Princeton University, Princeton, New Jersey 08543, USA*
[2]*University of Texas at Austin, Austin, Texas 78712, USA*
[3]*Brigham Young University, Provo, Utah 84602, USA*

(Received 2 December 2012; accepted 11 March 2013; published online 21 May 2013)

Transverse dipole and quadrupole modes have been excited in a one-component cesium ion plasma trapped in the Paul Trap Simulator Experiment (PTSX) in order to characterize their properties and understand the effect of their excitation on equivalent long-distance beam propagation. The PTSX device is a compact laboratory Paul trap that simulates the transverse dynamics of a long, intense charge bunch propagating through an alternating-gradient transport system by putting the physicist in the beam's frame of reference. A pair of arbitrary function generators was used to apply trapping voltage waveform perturbations with a range of frequencies and, by changing which electrodes were driven with the perturbation, with either a dipole or quadrupole spatial structure. The results presented in this paper explore the dependence of the perturbation voltage's effect on the perturbation duration and amplitude. Perturbations were also applied that simulate the effect of random lattice errors that exist in an accelerator with quadrupole magnets that are misaligned or have variance in their field strength. The experimental results quantify the growth in the equivalent transverse beam emittance that occurs due to the applied noise and demonstrate that the random lattice errors interact with the trapped plasma through the plasma's internal collective modes. Coherent periodic perturbations were applied to simulate the effects of magnet errors in circular machines such as storage rings. The trapped one component plasma is strongly affected when the perturbation frequency is commensurate with a plasma mode frequency. The experimental results, which help to understand the physics of quiescent intense beam propagation over large distances, are compared with analytic models. © *2013 AIP Publishing LLC*.
[http://dx.doi.org/10.1063/1.4804408]

I. INTRODUCTION

The stable transport of intense charged-particle beams over large distances in magnetic alternating-gradient particle accelerator systems[1–6] can be adversely affected by coherent periodic perturbations that can be created in ring machines wherein a circulating charge bunch experiences the deleterious effects of a magnet error repeatedly as it travels around the ring. Propagating charge bunches can also be affected by random misalignments of the magnets, or random errors in the magnet strength or spacing.[7,8] The experimental results presented in this paper demonstrate that these forms of lattice noise interact with the charge bunch through their coupling to the collective modes of the charge bunch.

Magnetic alternating-gradient transport systems are used in particle accelerators to provide transverse confinement of the charge bunch while they are accelerated to high energy, or stored in rings. These transport systems use a periodic lattice of quadrupole magnets that generate a $\boldsymbol{v}_z \times \boldsymbol{B}_\perp^{\rm ext}$ force that alternately accelerates the charge bunch towards or away from the axis, where $\boldsymbol{v}_z$ is the axial velocity of the beam particles and $\boldsymbol{B}_\perp^{\rm ext}$ is the perpendicular component of the externally applied magnetic field. Dynamic stability is achieved as long as the magnet strength is not so strong that it would eject particles from the system or as long as the magnets are not so far apart that the particles have time to drift to the wall. In order to study the dynamics of particle beams in large accelerator systems, many experimental studies have been carried out in compact, laboratory-scale, and experiments.[5,6,9–17] A linear Paul trap[18] is suitable for studying the transverse dynamics of such a system because the self-fields and spatially periodic force that a slice of a long charge bunch in the transport system experiences are the Lorentz transforms of the self-field and time oscillating electrostatic force that a long trapped charge column experiences in a linear Paul trap. The transverse dynamics of particles in the two systems are equivalent.[6,9–13,19–21]

The Paul Trap Simulator Experiment (PTSX) device[9] is a linear Paul trap and consists of three co-linear cylinders, as shown in Figure 1, with radius $r_w = 0.1$ m, each divided into four 90° azimuthal sectors, in a vacuum of 1×10^{-10} Torr. The pure cesium-ion collisionless plasma is confined radially in the central 2 m long cylinder by oscillating voltages (typically $V_0 = 150$ V, $f = 60$ kHz sinewaves). The outer two cylinders are each 0.4 m long and the voltage on these electrodes is held fixed at 50 V in order to confine the plasma axially. To inject

[a)]Paper GI3 6, Bull. Am. Phys. Soc. **57**, 111 (2012).
[b)]Invited speaker. Electronic address: egilson@pppl.gov. URL: http://nonneutral.pppl.gov.

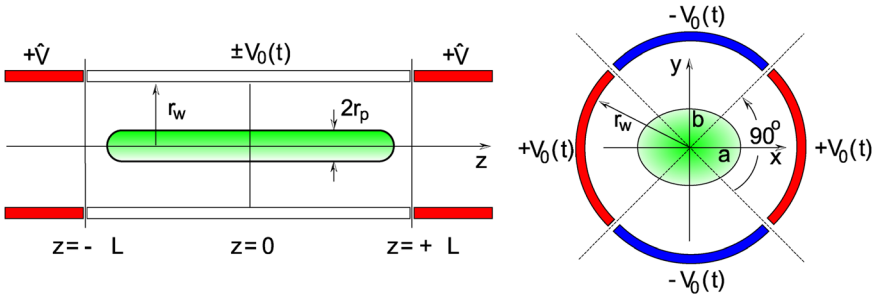

FIG. 1. The PTSX device consists of three cylindrical electrodes with radius $r_w = 0.1$ m, each divided into four 90° sectors. An oscillating voltage $\pm V_0(t)$ confines the plasma in the transverse plane to a radius r_p. Static voltages $+\hat{V}$ on the end electrodes confine the ions axially within a length $2L = 2$ m.

or dump the ions, the voltage on one or the other set of outer electrodes is switched to the same oscillating voltage that is applied to the central cylinder. The duration of injection (t_i), trapping (t_t), and dumping (t_d) may be varied independently with typical values being $t_i = 1.7$ ms, $t_t \leq 300$ ms, and $t_d \geq 10$ ms. A 5-mm diameter moveable circular copper collector measures the z-integrated radial charge profile when the charge bunch is dumped. The measured charge profile is time-averaged due to the slow axial drift speed of the ions. The time oscillating function $V(t)$ in PTSX corresponds to the spatially periodic magnetic quadrupole field strength gradient $B'(z)$ in the transport system. The rapidly oscillating quadrupole electric field near the axis of the apparatus gives rise to a ponderomotive force that is given by $\boldsymbol{F} = -m_b\omega_q^2\hat{r}$ where the average transverse focusing frequency is given by[1,9,22,23]

$$\omega_q = \frac{8e_bV_0}{m_br_w^2\pi f}\xi, \tag{1}$$

where $m_b = 133$ amu for Cs^+ ions in PTSX and r_w is the wall radius. The factor ξ depends on the shape of the voltage waveform and $\xi = 1/2\sqrt{2}\pi$ for a sinusoidal waveform $V(t)$. The ratio $\sigma_v^{sf} \equiv \omega_q/f$ is the smooth focusing phase advance and characterizes how many lattice periods there are for each oscillation corresponding to ω_q.

This paper reports detailed experimental studies of transverse dipole-mode and quadrupole-mode excitations in cesium ion plasmas trapped in the Paul Trap Simulator Experiment. Two arbitrary function generators were used to apply trapping voltage waveform perturbations with a range of frequencies and with either a dipole or quadrupole spatial structure. The experimental results demonstrate that harmonic perturbations applied with the correct spatial structure, and at the mode frequency, strongly perturb the plasma. Perturbations applied near $f + f_{\text{mode}}$ also excite the modes due to beating between the perturbation and the primary waveform with frequency f, but the effective strength of the excitation is smaller. Coherent periodic perturbations are simulated by changing the amplitude of every Nth lattice period of the applied voltage waveform. In this case, the plasma is strongly perturbed when the period of the perturbation is an integer multiple of either the dipole-mode or quadrupole-mode period, depending on the spatial structure of the perturbation. The data show that large-amplitude excitations are created. Experiments carried out using random noise with either a dipole or quadrupole spatial structure show that the noise strongly perturbs the plasma when the frequency spectrum of the noise contains a significant component at the mode frequency. For both coherent periodic perturbations and random noise perturbations, the deleterious effect of the perturbation can be eliminated by removing the component of the perturbation at the mode frequency corresponding to the spatial structure of the perturbation.

This paper is organized as follows. Section II provides a theoretical description of the dipole and quadrupole modes and discusses how the perturbations are generated in the experiment. Section III shows data that demonstrate the existence of the dipole and quadrupole modes in cesium ion plasmas trapped in PTSX. Section IV describes the results of experiments that simulate periodic coherent dipole and quadrupole perturbations as a charge bunch travels for many turns though a ring machine. The data in Sec. V show that random lattice noise interacts with the charge bunch through the excitation of collective modes. Conclusions are presented in Sec. VI.

II. DIPOLE AND QUADRUPOLE MODES

The long, thin charge column in PTSX and charge bunches in transport systems both support a wide variety of collective modes, and these modes can be studied in the contexts of different models. Analytic progress can be made if a Kapchinskij-Vladimirskij (KV) distribution is assumed in which the transverse charge density distribution of the charge bunch is taken to be uniform within an elliptical beam envelope with major and minor radii $a(t)$ and $b(t)$. The frequencies of surface modes with azimuthal mode number ℓ can be found in a KV Poisson-Vlasov smooth-focusing model in which the KV distribution is used and the time dependent periodic quadrupole lattice is replaced by a continuous focusing force.[1] Alternately, the KV smooth-focusing envelope model can be used to derive expressions for the frequencies of an $\ell = 0$ body mode and the $\ell = 2$ quadrupole mode.[2] If the fully time dependent quadrupole lattice waveform is used in the KV envelope model, numerical solutions for the matched envelope parameters can be found and perturbed to study the dependence of the $\ell = 2$ quadrupole mode frequency on the space charge parameter KT/ϵ, where K is the perveance of the charge bunch, $T = 1/f$ is the period of the lattice waveform, and ϵ is the emittance of the charge bunch. Note that when considering the space charge parameter KT/ϵ in the beam frame, it can be shown that the line charge $N = \int n(r)2\pi r\,dr$ takes the place, in a root-mean-squared equivalent sense, of the perveance K, where $n(r)$ is the transverse number density. Finally,

particle-in-cell (PIC) codes[24] can be used to create steady state, matched beam distributions that can be perturbed to study the collective mode frequencies numerically.

It is sufficient, here, to write down analytic expressions for the $\ell = 1$ dipole and $\ell = 2$ quadrupole modes obtained from the KV smooth-focusing models[1]

$$f_{\text{dipole}} = f_q = \frac{\omega_q}{2\pi}, \tag{2}$$

$$f_{\text{quadrupole}} = 2f_q\left(1 - \frac{3}{4}\hat{s}\right)^{1/2}, \tag{3}$$

where ω_q is the average transverse focusing frequency and $\hat{s} = \omega_p^2/2\omega_q^2$ is the normalized intensity parameter that is an alternative space charge parameter to KT/ϵ. The dipole mode corresponds to a bulk transverse displacement of the plasma column, while the quadrupole mode corresponds to an elliptical perturbation of the surface of the charge bunch.

In order for external perturbations to interact with these collective beam modes, both the spatial structure and the frequency of the perturbation must be the same as those of the collective mode. While the frequency of the perturbation can be directly controlled using the arbitrary function generators that create the waveform $V(t)$, the spatial structure of the perturbation must be controlled by changing which PTSX electrodes the perturbation is applied to. As described earlier, the oscillating quadrupole field is produced near the center of a cylinder that is divided into four 90° segments. When the four segments have voltages $\{+V_0, -V_0, +V_0, -V_0\}$ $\sin(2\pi ft)$ applied to them, the potential in the interior of the cylinder can be written as

$$V(r,\theta,t) = \sin(2\pi ft)\frac{4V_0}{\pi}\sum_{\ell=1}^{\infty}\left(\frac{r}{r_w}\right)^{2\ell}\frac{\sin(\ell\pi/2)}{\ell}\cos(2\ell\theta). \tag{4}$$

For the general case, where the four segments have voltages $\{V_1, V_2, V_3, V_4\}$ applied to them and the potential in the interior of the cylinder has the form $V(r,\theta) = \sum_{\ell=0}^{\infty} C_\ell (r/r_w)^\ell \cos(\ell\theta)$, the normalized amplitude of each multipole component can be written as $A_\ell = \frac{1}{4}\int_0^{2\pi} V(r_w,\theta)\cos(\ell\theta)$, where the normalization is chosen so that a set of voltages $\{+1, -1, +1, -1\}$ generates a quadrupole term with strength $A_2 = 1$. Given this convention, the set of voltages $\{+1, -1, +1, -1\}$ produces a quadrupole term $A_2 = 1$, a 12-pole term $A_6 = 1/3$, and higher-order terms.

To approximate a transverse dipole field near the center of the cylinder with $A_1 \neq 0$, the set of voltages $\{+1, 0, -1, 0\}$ can be applied. In this case, $A_1 = 1/2$, $A_3 = 1/6$, $A_5 = 1/10$, plus higher-order terms. In practice, it is simplest to create a dipole perturbation to a nominal quadrupole configuration by applying a small perturbation δ to a single electrode by choosing a set of voltages $\{+(1+\delta), -1, +1, -1\}$. This set of voltages can be easily decomposed as $\{+(1+\delta), -1, +1, -1\} = (1+\delta/4)\{+1, -1, +1, -1\} + \delta/2$ $\{+1, 0, -1, 0\} + \delta/4\{+1, +1, +1, +1\}$, that is, as the sum of a perturbed quadrupole configuration plus a dipole perturbation, and a uniform perturbation. In this case, $A_0 = \delta\pi/8$, $A_1 = \delta/4$, $A_2 = 1 + \delta/4$, $A_3 = \delta/12$, $A_5 = \delta/20$, $A_6 = 1/3 + \delta/12$. The effects of hexapole and higher order terms can be safely neglected because the trapped plasmas are confined near the center of the cylinder where $r/r_w < 0.25$. The $\delta/4$ increase in the quadrupole field can be compensated for by lowering the voltage amplitude on all four electrodes by $\delta/4$ if desired. Note that the A_0 term, corresponding to a uniform potential perturbation applied to the wall of the cylinder, does not contribute to the electrostatic force felt by ions in the trap. Experiments were carried out in which uniform potential perturbations were applied to the trap walls for a variety of system parameters, and the results confirmed that there was no effect on the plasma.

III. HARMONIC PERTURBATIONS

To study transverse dipole and quadrupole modes excited in trapped charge bunches in PTSX, experiments were carried out in which a harmonic perturbation was added to the nominal sinusoidal confining voltage waveform. A sinusoidal confining voltage waveform is typically used because the high frequency components of more realistic square waveforms are difficult to pass through the PTSX amplifier system. Initial experiments using small amplitude perturbations with frequencies near mode frequencies caused a loss of the charge bunch that was too rapid to characterize well. It was too difficult to operate at lower perturbation amplitude due to the poor perturbation amplitude resolution available when using the 12 bit digital to analog converter of the arbitrary function generator. Therefore, an alternative method of applying a harmonic perturbation was used in which the frequency of the perturbation is chosen to be near $f + f_{\text{mode}}$ so that the drive at the mode frequency due to beating between the primary waveform with frequency f and the effective perturbation would be smaller in amplitude.

The results are shown in Figure 2 for the cases of a dipole perturbation and a quadrupole perturbation. As

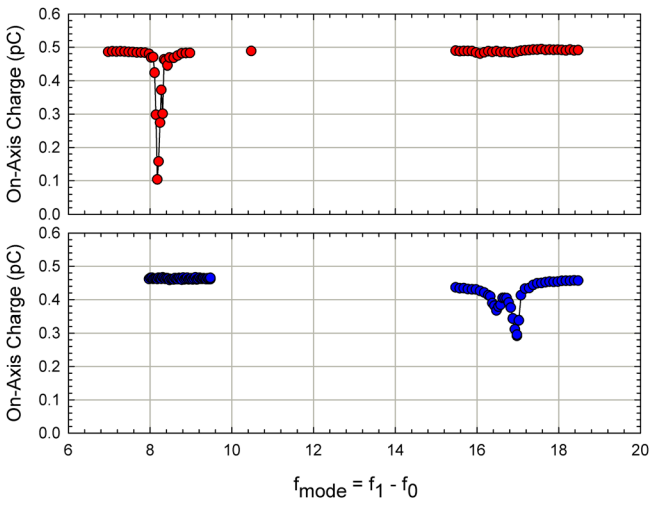

FIG. 2. (Top) When a dipole perturbation is applied, the charge bunch responds strongly near 8.4 kHz, the expected dipole mode frequency. There is little response near 16.8 kHz, the expected quadrupole mode frequency. (Bottom) Conversely, when a quadrupole perturbation is applied, the charge bunch responds strongly near the expected quadrupole mode frequency and not near the expected dipole mode frequency.

expected, when the spatial structure and frequency of the perturbation match those of a collective mode, the mode is excited to large amplitude. Once the perturbation is turned off, the energy in the excited mode causes the charge bunch to expand radially and the on-axis charge to decrease. The mode frequencies are near the predicted values using the simple model. The exact transverse focusing frequency is approximately 3% larger than the average transverse focusing frequency ω_q for the parameters used here, but this does not fully bring the predicted value into agreement with the observed value. Note that there are two peaks near the mode frequency in the case of the quadrupole perturbation and this is likely due to coupling to other modes that have frequencies near $2f_q$.

The data in Figure 3, taken in the neighborhood of the quadrupole mode frequency, are obtained with higher frequency resolution. These data show that, in fact, there is a rich spectrum of peaks near the quadrupole mode frequency. It is not clear whether the response of the charge bunch to the perturbation in this case is due to higher-order multipole components of the confining field exciting multipole-modes, or nonlinear coupling of the quadrupole drive to the charge bunch.

The space charge dependence of the quadrupole mode frequency was measured by repeating the experiment for various amounts of injected charge. The frequency of the primary peak in data such as those in Figure 3 is plotted as a function of the normalized intensity parameter $\hat{s}$ in Figure 4. The data do not agree well with the simple formula in Eq. (3), and so two-dimensional WARP particle-in-cell simulations were carried out with input parameters corresponding to the values used in the experiment. The simulation results, also displayed in Figure 4, show the frequency at which the maximum emittance growth occurred as a function os $\hat{s}$. Note that while both the experimental data and the simulation results have a weak dependence on $\hat{s}$, there is a systematic difference between them. This difference may be explained by the uncertainty in several of the experimental parameters.

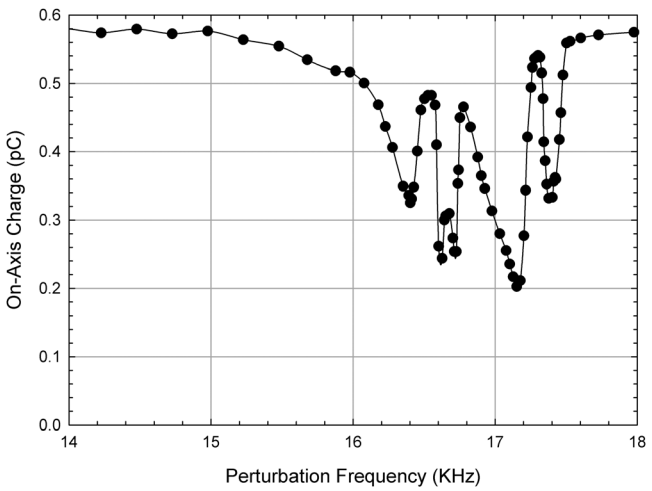

FIG. 3. A quadrupole perturbation generates a strong response in the charge bunch and leads to plasma loss at many frequencies in the neighborhood of the quadrupole mode frequency.

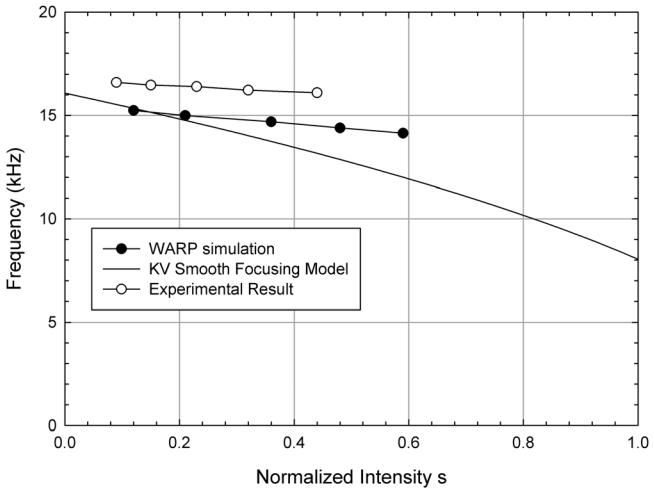

FIG. 4. A simple KV smooth-focusing model predicts a decrease in the quadrupole mode frequency as a function of the normalized intensity parameter $\hat{s}$. However, both the experimental data and the results of 2D WARP particle-in-cell simulations exhibit a weak dependence on $\hat{s}$.

IV. COHERENT PERIODIC RESONANCES

In a ring machine, the charge bunch circulates many times and therefore will experience lattice perturbations in a coherent periodic fashion. For example, a quadrupole magnet in an otherwise regular magnetic lattice may be different in order to accommodate a beam injection or extraction section. If the circulating charge bunch travels around the ring with frequency f_{ring} and there simultaneously exists a transverse mode excitation with frequency f_q, then when $f_q = \nu f_{\text{ring}}$, for an integer ν, the adverse effect of the perturbation may be compounded with each transit of the charge bunch around the ring. The integer ν is called the tune of the transport system, and avoiding integer tunes will avoid the adverse effects of dipole modes interacting with coherent periodic lattice errors. Correspondingly, for the quadrupole mode that has a frequency near $2f_q$, avoiding both half-integer and whole-integer tunes will avoid the adverse effects of the interaction of the coherent periodic perturbation with the collective mode.

In the experiments carried out on PTSX, coherent period perturbations were implemented by changing the waveform voltage amplitude of every Nth lattice period by a fixed amount, corresponding to a ring with N lattice periods around its circumference. The size of this perturbation of every Nth lattice period is called the noise amplitude and is described as a percentage of the unperturbed waveform voltage amplitude V_0. For example, LHC has approximately 200 lattice periods in its circumference, while the SNS storage ring has 24. In some experiments the perturbation was applied to all four PTSX electrodes to create coherent periodic perturbations with a quadrupole spatial structure, and in other experiments the perturbation was applied to a single PTSX electrode to create a predominantly dipole perturbation.

For both dipole and quadrupole perturbations, the dependence on the ring periodicity N is studied by first adjusting the PTSX operating parameters to ensure a tune of $\nu = 2$ for $N = 12$ given a fixed lattice frequency of 60 kHz. This adjustment is accomplished by varying the waveform

voltage amplitude V_0 in the neighborhood of values corresponding to an estimate for $\nu = 2$. The desired tune is found when V_0 is chosen such that the measured on-axis charge of the trapped charge bunch decreases significantly. Indeed, *a posteriori* calculation of the smooth-focusing vacuum phase advance gives 58° which corresponds to an exact vacuum phase advance of 60° and a tune of $\nu = 2$. For dipole perturbations, the dipole mode frequency is then 10 kHz, while for quadrupole perturbations, the quadrupole mode frequency is then 20 kHz. The data in Figure 5 demonstrate that, for quadrupole perturbations, the adverse effect of the perturbation is strong when the tune ν is an half- or whole-integer value. Similarly, data for dipole perturbations show that the adverse effect is strong when the tune ν is a whole-integer value. Similar data were obtained for a vacuum phase advance of 45° for which the dipole mode period is 8 lattice periods.

The tune ν can be changed by varying the mode frequency rather than by changing the periodicity of the ring. Experiments were carried out for both dipole and quadrupole perturbations in which the periodicity of the lattice is fixed at $N = 12$, while the waveform voltage amplitude V_0 is varied from 0 V to over 350 V. In the absence of resonant mode excitation, the measured on-axis charge as a function of waveform voltage amplitude should be small for small values of V_0 since the ponderomotive confining force is small. The measured signal should then increase with V_0 as the transverse confinement becomes stronger until V_0 is large enough that the vacuum phase advance exceeds 180° and single particle confinement is lost. Indeed, the data in Figures 6 and 7 show that this is the case, with the added structure of the resonant mode excitations. The data in Figure 6 are equivalent to data in Ref. 11, while the data in Figure 7 are for dipole perturbations.

The perturbed waveform, a periodic sine wave that has a different amplitude every 12th period, has a frequency spectrum that includes components at multiples of 5 kHz. The perturbation thus acts on the trapped charge bunch by exciting either the dipole mode at 10 kHz or the quadrupole mode

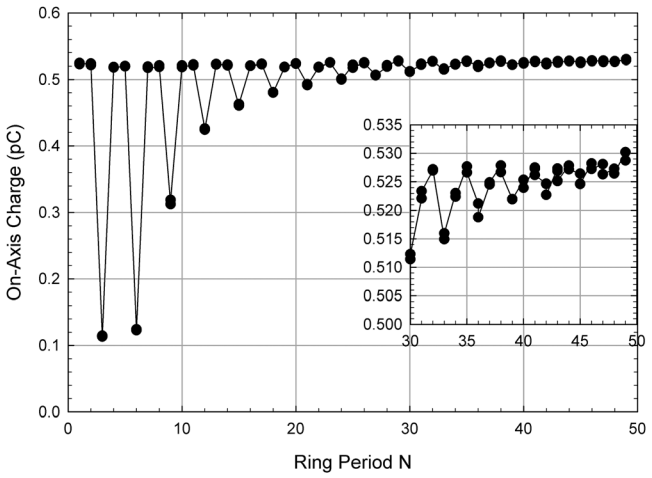

FIG. 5. For a vacuum phase advance $\sigma_v = 60°$, the quadrupole mode period is three lattice periods. Therefore, whenever the ring period N is a multiple of three, the quadrupole mode is strongly excited. The inset shows a magnified view of the data above $N = 30$ in order to demonstrate that the effect is still seen up to $N = 50$.

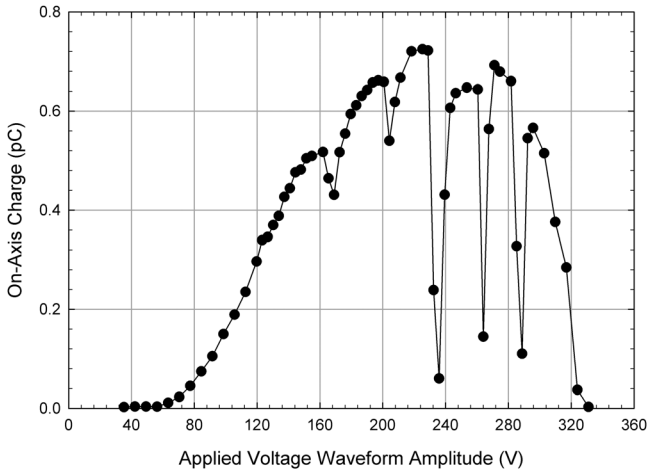

FIG. 6. When a 2% quadrupole perturbation is applied, half- and whole-integer resonances are seen as the quadrupole mode frequency changes, while the waveform voltage amplitude is swept from 40 V to 350 V. Above 350 V, single particle dynamic stability is lost.

at 20 kHz, depending on the spatial structure of the applied perturbation. Experiments in which the perturbed waveform is filtered to remove certain frequency components before it is applied to the PTSX electrodes demonstrated that if the 10 kHz component is removed, in the dipole case, the deleterious effect of the perturbation is nearly eliminated; the perturbation reduces the measured on-axis charge from 0.55 pC to 0.05 pC, and eliminating the 10 kHz component of the perturbation restores the signal to 0.40 pC. However, due to the finite strength of the perturbation, the 50 kHz and 70 kHz component, both of which beat with the primary lattice frequency $f = 60$ kHz to drive the dipole mode, must be removed from the spectrum as well in order to fully eliminate the effect of the perturbation to 0.55 pC. A similar result was obtained for the quadrupole case, where frequencies of 20 kHz, 40 kHz, and 80 kHz were removed and the effect of the perturbation was eliminated. Figure 8 shows the applied voltage waveform after the harmful frequency components have been removed in the case of the dipole perturbation.

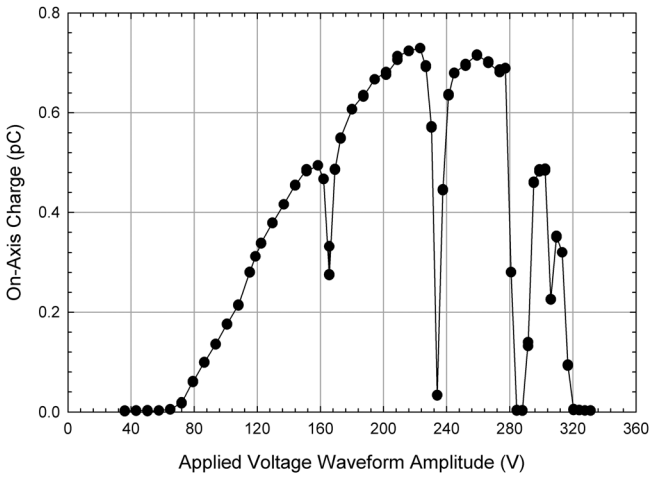

FIG. 7. When a 2% dipole perturbation is applied, integer resonances are seen as the dipole mode frequency changes, while the waveform voltage amplitude is swept from 40 V to 350 V. Above 350 V, single particle dynamic stability is lost.

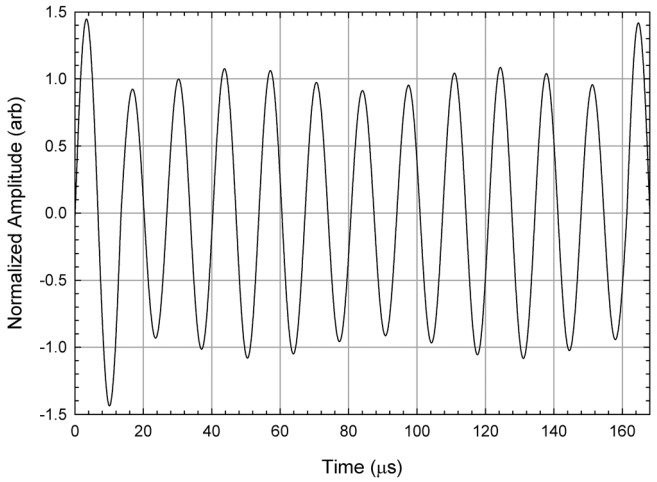

FIG. 8. A waveform in which a 60 kHz waveform of unit amplitude where every 12th period has amplitude 1.5 has had the 10 kHz, 50 kHz, and 70 kHz components removed. Such a waveform will not drive the dipole mode at 10 kHz.

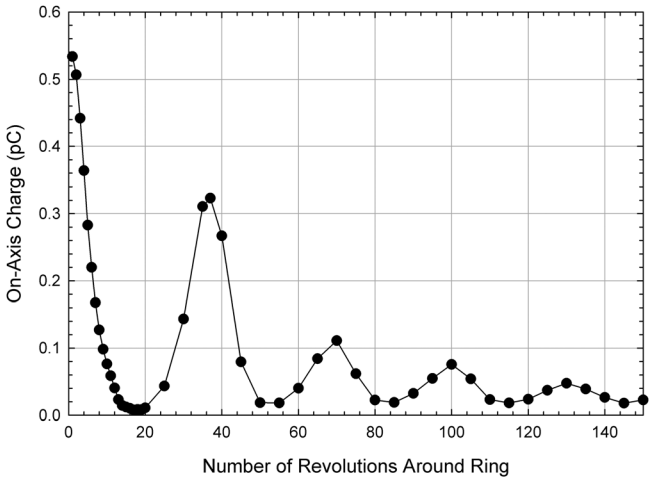

FIG. 10. The duration dependence of a coherent periodic dipole perturbation with $N = 12$ and a 6% amplitude is not monotonic. This suggests the mode is driven into a nonlinear regime.

It may therefore be possible to carefully alter the strengths of quadrupole magnets in a ring machine to compensate for the adverse effect of a single magnet.

Variation of the amplitude or the duration of the perturbation for a ring periodicity $N = 12$ and a tune $\nu = 2$ corresponding to a vacuum phase advance of 60° shows that these modes are driven to amplitudes that are sufficiently large to see the effects of different nonlinearities. For a nonlinear oscillator without damping, a constant amplitude drive at the linear mode frequency causes the oscillator amplitude to periodically increase and decrease with a frequency that depends on the strength of the drive, and the strength and type of the nonlinearity. If the perturbation duration and amplitude used in a PTSX experiment are such that the mode amplitude is large when the perturbation is turned off, the charge bunch relaxation process will cause the energy in the mode to increase the effective transverse temperature, broaden the plasma and decrease the on-axis number density. Conversely, if the perturbation is turned off when the mode amplitude is small, the relaxation process will not significantly change the plasma parameters.

Typical data are shown in Figure 9 where the on-axis charge does not decrease monotonically as the perturbation amplitude increases for the case of a dipole excitation. Similarly, the data in Figure 10 show that the decrease in on-axis charge does not decrease monotonically as a function perturbation duration at fixed perturbation amplitude. The perturbation amplitudes and durations corresponding to the locations of minimum on-axis charge are plotted in Figure 11 along with best-fit lines showing that the location of these minima scales as the product of the perturbation amplitude and duration raised to the power $-5/4$. This scaling is consistent with the $(r/r_w)^6$ 12-pole correction to the harmonic ponderomotive potential. It is not consistent with quartic correction to the harmonic ponderomotive potential due to the image charge effect that would instead give rise to a $-3/2$ scaling.

For the case of a quadrupole perturbation, a non-monotonic decrease in the on-axis charge as a function of

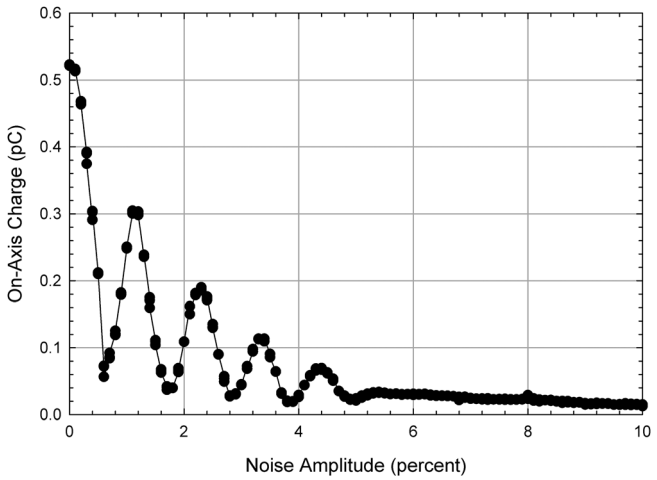

FIG. 9. The amplitude dependence of a coherent periodic dipole perturbation with $N = 12$ applied for 1800 lattice periods is not monotonic. This suggests the mode is driven into a nonlinear regime.

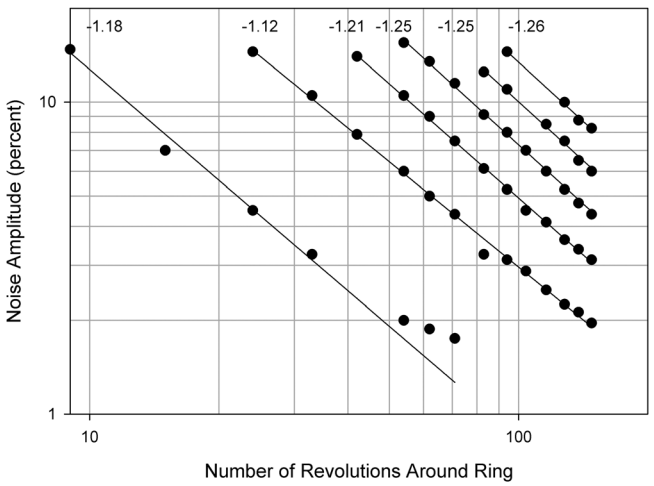

FIG. 11. The locations of the minima extracted from datasets such as those in Figures 9 and 10 scale as the product of the perturbation amplitude and duration raised to the power $-5/4$. The slope of each best-fit line is shown near the top of each line.

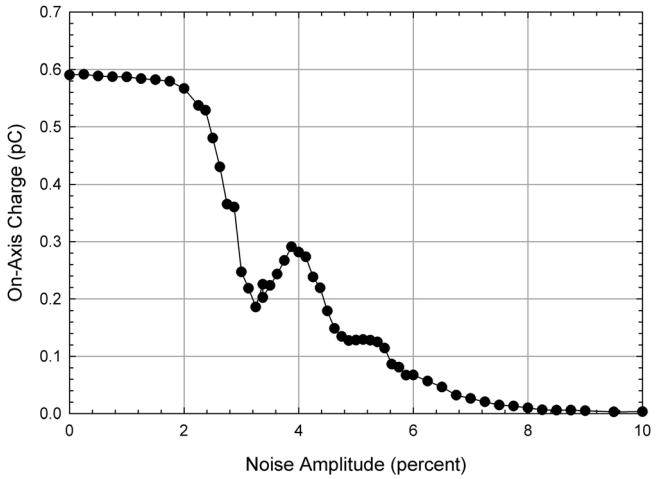

FIG. 12. The amplitude dependence of a coherent periodic quadrupole perturbation with $N = 12$ applied for 1800 lattice periods is not monotonic. This suggests the mode is driven into a nonlinear regime.

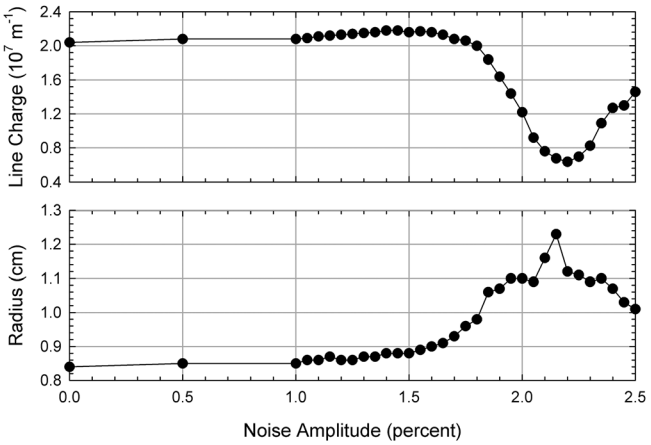

FIG. 14. (top) The line charge decreases at first, but then increases at larger perturbation amplitudes. The apparent loss may be due to particles falling below the detection threshold of the diagnostic. (bottom) The root-mean-squared radius increases at first, but then decreases at larger perturbation amplitude.

both amplitude at fixed duration (Figure 12), and also duration at fixed amplitude is also seen. Here, however, the scaling of the location of the minimum measured values scales as the $-3/4$ power of the product of perturbation amplitude and duration (Figure 13). Quadrupole perturbations do not move the charge bunch centroid, and so image charge effects and higher order trap multipole effects are not expected to be the source of the nonlinearity. Rather, it is the space-charge that is likely to be the source of the nonlinearity.

To better characterize the effect of the quadrupole coherent periodic perturbation, complete radial plasma density profiles were measured as a function of the perturbation amplitude. The on-axis charge measurement for each profile is what is used in data such as those in Figure 12. However, the line charge and root-mean-squared radius can now also be computed from the radial plasma density profiles. The results in Figure 14 show that, as expected, the line charge decreases at first while the radius increases. Somewhat surprisingly, the line charge begins to increase at larger values of the perturbation amplitude. It is possible that, when large amplitude modes are excited, after the charge bunch relaxes when the perturbation is shut off, a large number of particles fall below the detection threshold of the measurement. It may also be possible that particle loss occurs only during the relaxation after the perturbation is shut off.

The dependence of the effect of the quadrupole coherent periodic perturbation on space charge was measured by varying the amount of injected charge. Trapped charge bunches with normalized intensities of $\hat{s} = 0.08$, 0.20, and 0.31 were created, trapped, and subjected to quadrupole coherent periodic perturbations of different amplitudes. The data in Figure 15, including the data replotted from Figure 12 for $\hat{s} = 0.20$, show that the perturbation amplitudes at which the minima occur varies as a function of $\hat{s}$. As space charge increases, the minima shift to larger values of the perturbation amplitude, which is consistent with a nonlinearity due to space charge.

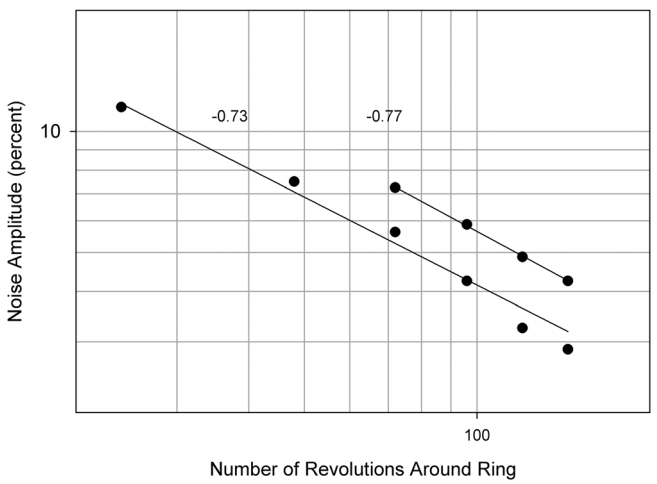

FIG. 13. The locations of the minima extracted from datasets such as those in Figure 12 scale as the product of the perturbation amplitude and duration raised to the power $-3/4$. The slope of each best-fit line is shown near the top of each line.

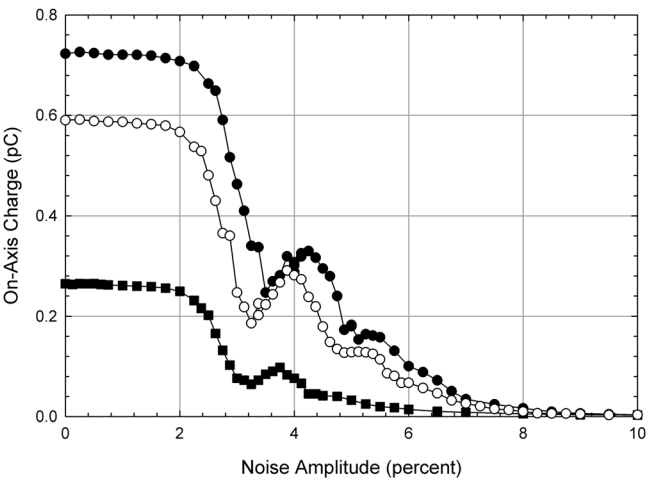

FIG. 15. The perturbation amplitudes at which the minima occur varies as a function of $\hat{s}$ for $\hat{s} = 0.08$, 0.20, and 0.31.

V. RANDOM NOISE

The quadrupole magnets in an alternating-gradient accelerator system may each have a random transverse misalignment, and this leads to a dipole magnetic field error in the direction of the misalignment. Variations in the strength of the quadrupole magnets leads to a quadrupole error. In either case, the error can be characterized by a number Δ_n for each of n magnets in a lattice. For the experiments presented here, Δ_n are chosen from a Gaussian distribution of unit variance and a given amplitude. In PTSX, where a sinusoidal waveform is used, the amplitude of the nth half-period of the waveform is taken to be $V_0(1+\Delta_n)$. In this case, the amplitude of the Gaussian distribution from which the Δ_n are selected is called the noise amplitude and is described as a percentage of the unperturbed waveform voltage amplitude V_0. After the ions are injected into PTSX, they are allowed to relax for 1200 lattice periods, then the noisy perturbation is applied for up to 1800 lattice periods, and finally they relax for another 3000 lattice periods. At the end of the trapping time, the ions are dumped onto the collector which measures the on-axis charge which is used to infer the on-axis number density of the previously trapped charge bunch.

Previous experiments demonstrated the effects of random quadrupole noise on a trapped plasma with moderate space charge intensity $\hat{s} \sim 0.2$.[25,26] In those experiments, the duration of the perturbation was increased for noise amplitudes of 0.5%, 1.0%, and 1.5%, and, in each case, the effect of the noise increased with perturbation duration. The effect of the noise also increased, at a given perturbation duration, with the perturbation amplitude. For example, a noise amplitude of 1.0% applied for 1800 lattice periods lead to a doubling of the inferred transverse emittance of the charge bunch. It is important to note that the data presented in Refs. 25 and 26 were obtained by choosing a noise amplitude and duration, and then repeatedly generating the list of random numbers Δ_n to measure the range of possible outcomes. After characterizing the range of possible outcomes, a set of Δ_n was selected that gave the average outcome. Thus, the data presented in Refs. 25 and 26 correspond to the average effect of quadrupole noise of a given strength and duration.

If the perturbation is applied to one of the four PTSX electrodes, then the perturbation is predominantly dipolar. The data in Figure 16 show that a doubling of the inferred transverse emittance occurs for only 0.5% amplitude dipole noise. These data show the average effect of the noise at a given setting. It is not surprising that a smaller amplitude perturbation is needed since the dipole field is non-zero near the axis, while the quadrupole field approaches zero on the axis. Nevertheless, both dipole and quadrupole perturbations lead to increases in the radius, effective transverse temperature and emittance of the charge bunch, and a decrease in the normalized intensity and, ultimately, a loss of charge. In order to verify that the results of the experiments in which the perturbation was applied to a single PTSX electrode were due to the effect of the dipole field, the experiment was repeated, but with either the quadrupole part of the perturbation removed or with only the quadrupole part and no dipole contribution. The results in Figure 17 clearly demonstrate

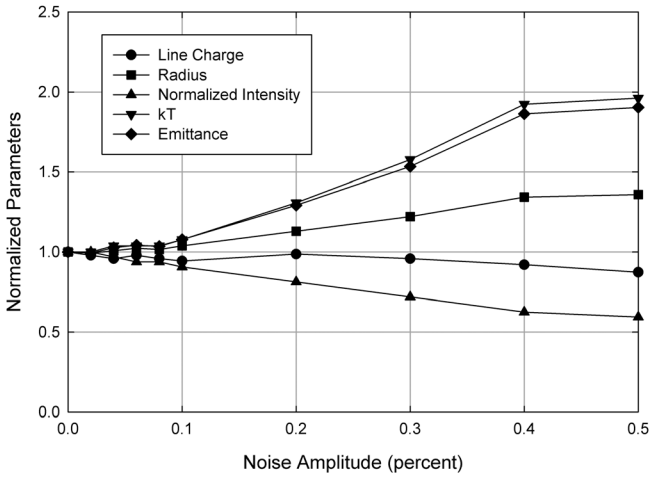

FIG. 16. A random noise perturbation applied to a single PTSX electrode for 1800 lattice periods causes the charge bunch radius, effective transverse temperature and emittance to increase, while the normalized intensity decreases.

that the effect of the perturbation applied to a single PTSX electrode is due to the dipole field because removing the quadrupole component does not change the result, while applying only the quadrupole component does not affect the charge bunch. Note that this is due the small effective strength of the quadrupole perturbation in this case.

For a dipole perturbation strength of 0.5% and a duration of 1800 lattice periods, a set of random number Δ_n was selected that led to a significant decrease in the measured on-axis charge from 0.4 pC to 0.1 pC. The spectrum of the perturbed waveform was then modified by removing all frequency components from zero up to a frequency f. The 1800 lattice period duration of the perturbation corresponds to a 30 ms duration so that the frequency resolution of the Fourier transform of the waveform is $\delta f = 33.3$ Hz. The maximum frequency in the spectrum is 10 MHz, due to the 50 ns clock time of the arbitrary function generator. In Figure 18, it is shown that the damaging effect of the dipole noise is eliminated, and the measured on-axis charge returns to the

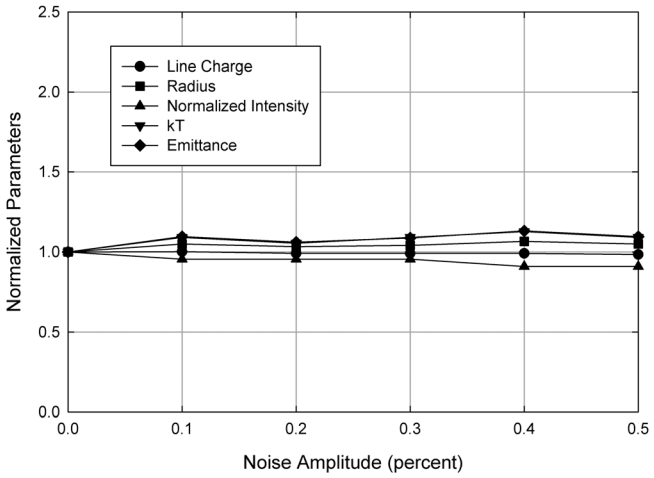

FIG. 17. The quadrupole component of the noise signal applied to a single PTSX electrode can be applied separately and has no effect on the trapped charge bunch. This demonstrates that the effect of noise applied to a single PTSX electrode is due to the dipole component.

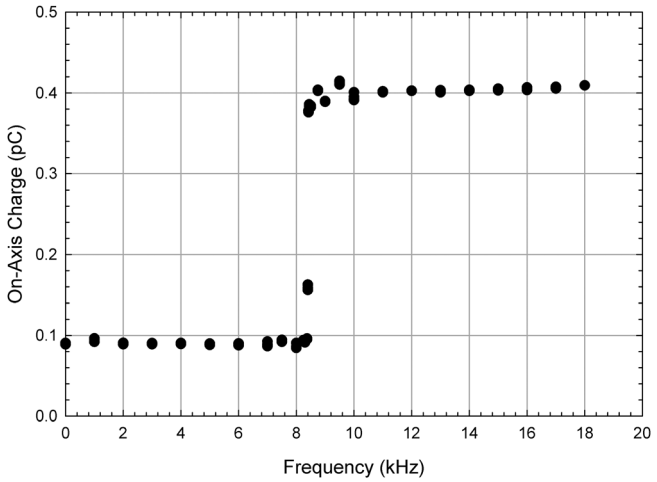

FIG. 18. A low-pass filter removes all frequency components less than f and when the component at 8.400 kHz is removed, the damaging effect of the dipole noise is eliminated.

unperturbed value of 0.4 pC, when the filter eliminates the frequency component at 8.400 kHz, corresponding to the dipole mode frequency. Moreover, no further increase in the on-axis charge is observed if the filter also removes frequency components near the quadrupole mode frequency near $2f_q$. The data in Figure 19 show the measured on-axis charge when individual 33.3 Hz-wide frequency components are removed from the Fourier spectrum before the perturbed waveform is applied. The width of the peak is $\Delta f/f_q = 0.4\%$.

The analogous set of experiments for a quadrupole perturbation with a strength of 1.0% and a duration of 1800 lattice periods was also carried out and the result is shown in Figure 20. As the width of the filter window is increased, the increase in the on-axis charge measurement is more gradual than in the dipole case and also exhibits a plateau above 17.5 kHz. These results demonstrate that there is a pair of comparatively broad peaks at 16.4 kHz and 16.9 kHz, near the quadrupole mode frequency $2f_q$. Their breadth implies that removing individual 33.3 Hz-wide frequency components from the Fourier spectrum is not sufficient

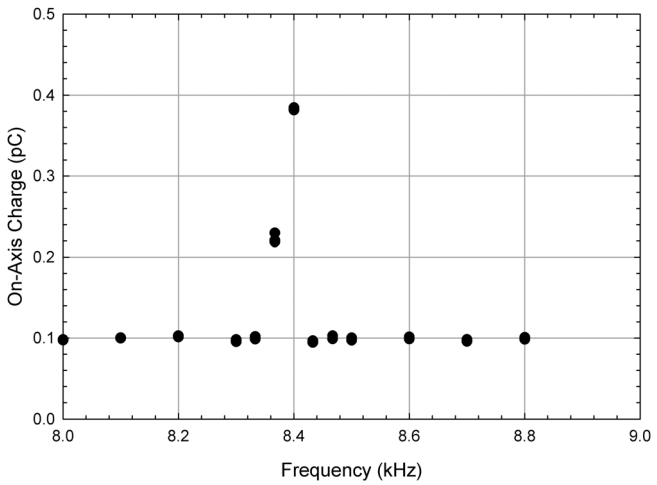

FIG. 19. Removing individual 33.3 Hz-wide frequency components from the spectrum of the noise perturbation reveals that the dipole mode has a fractional width $\Delta f/f_q = 0.4\%$.

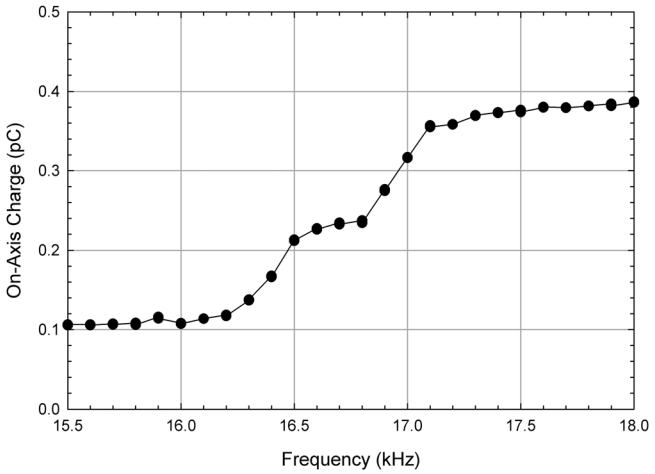

FIG. 20. A low-pass filter removes all frequency components less than f and when all components less than 17.5 kHz are removed, the damaging effect of the quadrupole noise is eliminated.

to eliminate the adverse effect of the quadrupole noise. However, a 1 kHz-wide band of frequencies centered at 16.75 kHz can be removed to restore the on-axis charge to its unperturbed value.

While filtering of the waveform applied to the PTSX electrodes is simple, filtering the spectrum of errors in a set of quadrupole magnets may be rather difficult. Instead of filtering the Fourier spectrum, then, it is possible to change the spectrum by manipulating the signal in the time domain by re-ordering the numbers in a given list Δ_n. For example, a list of 3600 random numbers Δ_n that gives rise to a large Fourier component at the dipole mode frequency 8.400 kHz was re-ordered randomly approximately 1000 times until an ordering was found that gives rise to a waveform with near-zero component at 8.400 kHz. Simply sorting the list of numbers Δ_n would also suffice to eliminate the frequency component at the mode frequency, indeed many mode frequencies simultaneously, but could lead to an undesirable gradual change in the average transverse focusing frequency.

VI. CONCLUSIONS

Both transverse dipole and quadrupole modes have been excited in trapped pure-cesium ion plasmas in PTSX. These modes can be excited by perturbations with the correct spatial structure and either: harmonic perturbations at the mode frequencies, coherent periodic perturbations with frequency components at the mode frequencies, or random noise with frequency components at the mode frequencies. Harmonic perturbations were used to excite and characterize the modes in the PTSX apparatus. Coherent periodic perturbations can be found in ring machines when a circulating beam bunch passes each revolution through a magnet set with an error. The deleterious effect of the error on the charge bunch when the tune ν is a half-integer (for quadrupole) or whole-integer (for quadrupole or dipole), can be eliminated by removing the components of the perturbation that are the mode frequencies. Nonlinearities in accelerator systems may be characterized by measuring the effects of errors on the beam bunch as a function of perturbation duration, or equivalently,

the number of times the bunch propagates around the ring. The effects of random dipole and quadrupole lattice noise can be mitigated by removing frequency components of the noise at the mode frequencies. If the errors in individual magnet sets are well-characterized, and do not change in time, it is possible to re-order the magnet sets to accomplish this.

ACKNOWLEDGMENTS

This research was supported by the U.S. Department of Energy.

[1]R. C. Davidson and H. Qin, *Physics of Intense Charged Particle Beams in High Intensity Accelerators* (World Scientific, Singapore, 2001).
[2]M. Reiser, *Theory and Design of Charged Particle Beams* (Wiley, New York, 1994).
[3]A. W. Chao, *Physics of Collective Beam Instabilities in High Energy Accelerators* (Wiley, New York, 1993).
[4]See, for example, in *Proceedings of the 2003 Particle Accelerator Conference*, IEEE Catalog Number 01CH37423, pp. 1–3571 (2003).
[5]P. G. O'Shea, M. Reiser, R. A. Kishek, S. Bernal, H. Li, M. Pruessner, V. Yun, Y. Cui, W. Zhang, Y. Zou *et al.*, Nucl. Instrum. Methods Phys. Res. A **464**, 646 (2001).
[6]N. Kjærgaard and M. Drewsen, Phys. Plasmas **8**, 1371 (2001).
[7]C. L. Bohn and I. V. Sideris, Phys. Rev. Lett. **91**, 264801 (2003).
[8]F. Gerigk, Phys. Rev. ST Accel. Beams **7**, 064202 (2004).
[9]E. P. Gilson, R. C. Davidson, P. C. Efthimion, and R. Majeski, Phys. Rev. Lett. **92**, 155002 (2004).
[10]H. Okamoto and H. Tanaka, Nucl. Instrum. Methods Phys. Res. A **437**, 178 (1999).
[11]S. Ohtsubo, M. Fujioka, H. Higaki, K. Ito, H. Okamoto, H. Sugimoto, and S. M. Lund, Phys. Rev. ST Accel. Beams **13**, 044201 (2010).
[12]H. Takeuchi, K. Fukushima, K. Ito, K. Moriya, H. Okamoto, and H. Sugimoto, Phys. Rev. ST Accel. Beams **15**, 074201 (2012).
[13]N. Kjærgaard, K. Mølhave, and M. Drewsen, Phys. Rev. E **66**, 015401 (2002).
[14]B. Beaudoin, I. Haber, R. Kishek, S. Bernal, T. Koeth, D. Sutter, P. O'Shea, and M. Reiser, Phys. Plasmas **18**, 013104 (2011).
[15]K. W. Murch, K. L. Moore, S. Gupta, and D. M. Stamper-Kurn, Phys. Rev. Lett. **96**, 013202 (2006).
[16]U. Schramm, T. Schätz, and D. Habs, Phys. Rev. E **66**, 036501 (2002).
[17]A. Valishev, S. Nagaitsev, V. Kashikhin, and V. Danilov, in *Proceedings of the 2011 Particle Accelerator Conference* (2011), p. 1606.
[18]W. Paul and H. Steinwedel, Z. Naturforsch. A **8**, 448 (1953).
[19]R. C. Davidson, H. Qin, and G. Shvets, Phys. Plasmas **7**, 1020 (2000).
[20]R. Takai, H. Enokizono, K. Ito, Y. Mizuno, K. Okabe, and H. Okamoto, Jpn. J. Appl. Phys. **45**, 5332 (2006).
[21]K. Ito, K. Nakayama, S. Ohtsubo, H. Higaki, and H. Okamoto, Jpn. J. Appl. Phys., Part 1 **47**, 8017 (2008).
[22]E. P. Gilson, R. C. Davidson, P. C. Efthimion, R. Majeski, and H. Qin, Laser Part. Beams **21**, 549 (2004).
[23]E. P. Gilson, R. C. Davidson, P. C. Efthimion, R. Majeski, and H. Qin, in *Proceedings of the 2003 Particle Accelerator Conference*, IEEE Catalog No. 03CH37423C (2003), p. 2655.
[24]A. Friedman, D. P. Grote, and I. Haber, Phys. Fluids B **4**, 2203 (1992).
[25]M. Chung, E. P. Gilson, R. C. Davidson, P. C. Efthimion, and R. Majeski, Phys. Rev. Lett. **102**, 145003 (2009).
[26]M. Chung, E. P. Gilson, R. C. Davidson, P. C. Efthimion, and R. Majeski, Phys. Rev. ST Accel. Beams **12**, 054203 (2009).